PRESENT ACHIEVEMENT AND FUTURE POSSIBILITY OF FATIGUE LIFE SIMULATION TECHNOLOGY FOR RC BRIDGE DECK SLABS

Chikako FUJIYAMA*, Esayas GEBREYOUHANNES**, Koichi MAEKAWA***

The University of Tokyo*

The University of Tokyo **

The University of Tokyo***

ABSTRACT: Fatigue life of RC bridge deck slab is simulated with full 3D nonlinear finite element analysis which fully traces mechanical damage and plasticity under high cycle repetition of loads in use of logarithmic accelerated time integration. The damaging process under the wheel type moving load is described. The influencing factors, i.e., thickness of slab, reinforcement arrangement, pre-stressing level and traffic conditions are examined separately by controlling effective variables. In addition, effect of water is shown in fatigue analysis of a simple beam model. In this study, future possibility of this simulation technology is discussed in line with infrastructure management for real structures.

KEYWORDS: fatigue simulation technology, bridge deck slab, moving load, water effect

1. INTRODUCTION

Recent developments in the field of computer simulation technology have led to a renewed interest in fatigue problems of RC bridge deck slabs.

The topic itself is not the latest issue. Serious damages of RC slabs were reported in 1960's in Japan. Researchers installed the wheel type moving load testing machinary and conducted assorted experiments from 1980's. Based upon the results of these experimental studies, some specifications which are thought as influence factors of fatigue life such as minimum thickness of a slab and required reinforcement arrangement were renewed in design codes. As a result, numbers of reports related to slab damages have become smaller.

On the other hand, the method of quantitative assessment on each effective factor has never be established yet even though slabs are guaranteed a certain quality by the codes. Here, simulation system is required for assessing residual life of existing damaged slabs. By controlling effective variables systematically, useful index to judge the performance is derived. It surely helps to plan the most suitable maintenance for slabs in service. The authors also introduce the method to evaluate the effect of water in the current simulation system. This study shows one of the practical solutions for the life-assessment of infrastructures.

2. FATIGUE SIMULATION SYSTEM FOR RC STRUCTURES

The fatigue simulation system for RC structure proposed is based on the direct path integral scheme. Numerical simulation is conducted by tracing the evolution of microscopic material states at each moment with multi directional fixed crack model (Maekawa *et al.* 2003). This simulation system has been enhanced for fatigue analyses by using logarithmic integral method (Maekawa *et al.* 2006a). Damage degradation is expressed by incremental

plasticity and fracturing. The framework is made up with essential three constitutive models, compression, tension and crack shear, which treat the cumulative fatigue damaging and time dependency effects. Full-3D simulation system is based on these core models (figure 2.1).

3. BRIDGE DECK SLAB SIMULATION

3.1 Prototype

Figure 3.1 shows prototype simulation model. Main transverse span is 2.0m and longitudinal span along the traffic moving direction is 3.0m and thickness is 190mm. All lines of the slab edge are supported in vertical direction, but rotation is free. Designed slab thickness and reinforcement arrangement (table 3.1) is based on the current Japanese road bridge design code.

Three types of loading (table 3.2), static, fixed point pulsating and moving point are considered. Static capacity of this prototype with 100mm square loading section is 594.0kN, and the mid-span deflection at this maximum loading rate is 7.7mm.

After this ultimate point, slab fails in punching shear. Moving load is also applied 100mm width.
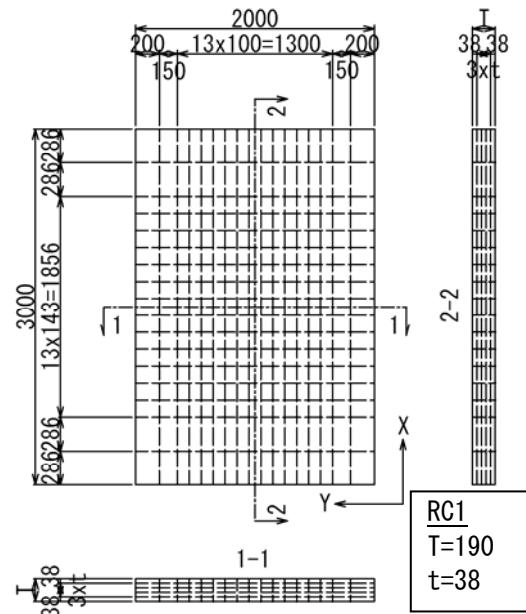

Figure 3.1 Prototype

Table 3.1 Reinforcement arrangement

arrangement	transverse	longitudinal
Upper side	D16 ctc 200	D16 ctc 260
Bottom side	D16 ctc 100	D16 ctc 130

Table 3.2 Loading patterns

Loading pattern	Period	Speed / Count
Static	---	0.02mm/min
Pulsating	0.12(s)	1 Loading - Unloading

	Compression model	Tension model	Crack shear model
Core Constitutive low	Stress-strain $\sigma = E_0 K_C \varepsilon_e$ $\varepsilon = \varepsilon_e + \varepsilon_p$	Stress-strain $\sigma = E_0 K_T \varepsilon_e$ $\varepsilon = \varepsilon_e + \varepsilon_p$	Shear stress-shear strain $\tau = \int_{-\pi/2}^{\pi/2} R_c'(\omega, \delta, \theta) \sin \theta d\theta$
Enhanced model for High cycle fatigue	Fracture parameter Kc considers time dependent plasticity & fracturing and cyclic fatigue damage $dK_C = \left(\frac{\partial K_C}{\partial t}\right)dt + \left(\frac{\partial K_C}{\partial \varepsilon_e}\right)d\varepsilon_e$ time dependent cyclic fatigue $\left(\frac{\partial K_c}{\partial \varepsilon_e}\right) = \lambda \sim when F_k = 0$ $\left(\frac{\partial K_c}{\partial \varepsilon_e}\right) = -\left(\frac{\partial F_k}{\partial \varepsilon_e}\right)\left(\frac{\partial F_k}{\partial K}\right) + \lambda \sim when F_k = 0$ $\lambda = K^3 \cdot (1 - K^4) \cdot g \cdot R$ El-Kachif and Maekawa 2004	Fracture parameter K_T considers time dependent fracturing and cyclic fatigue damage $dK_T = Fdt + Gd\varepsilon_e + Hd\varepsilon_e$ Time dependent fracturing Cyclic fatigue damage Maekawa et al. 2003, Hisasue 2005	Accumulated path function X reduce shear associated with cyclic fatigue damage $\tau = X \cdot \tau_0(\delta, \omega)$ function original model $X = 1 - \frac{1}{10}\log_{10}\left\{1 + \int |d(\delta/\omega)|\right\} \geq 0.1$ Contact density model by Li & Maekawa 1989 Modification of accumulated path function by Gebreyouhannes 2006
Physical meaning	Decrease of stiffness and plasticity accumulation by continuous fracturing of concrete	Decrease of tension stiffness by bond fatigue	Decrease of shear transfer normal to crack by continuous deterioration of rough crack surface

Figure 2.1 Fatigue simulation systems for RC structures

3.2 Failure under the moving load

Figure 3.2 shows the mid-span deflection under both pulsating and moving loads. The number of cycles where the deflection starts to increase rapidly is much different between two types of loading. Figure 3.3 presents S-N diagram of the prototype with fatigue life prediction formula by the JSCE code. Vertical axis is normalized by the static capacity. It is clear that the fatigue life under moving load is around 3 orders shorter than that under pulsating loads. This result is also observed in experimental studies (Matsui *et a*l. 1984,1987, Pekikaris *et al*. 1988, 1989).

It is tempting to pose basic question of the reason what promotes damage degradation under moving load. The element located under the moving load, 300mm outside of mid-span, half height of the total thickness is picked up. In the case of moving load, principal strain seems to exceed crack strain in early stage (figure 3.4). Furthermore, principal stress
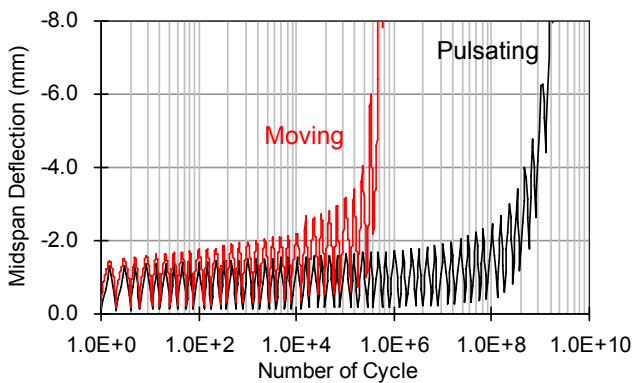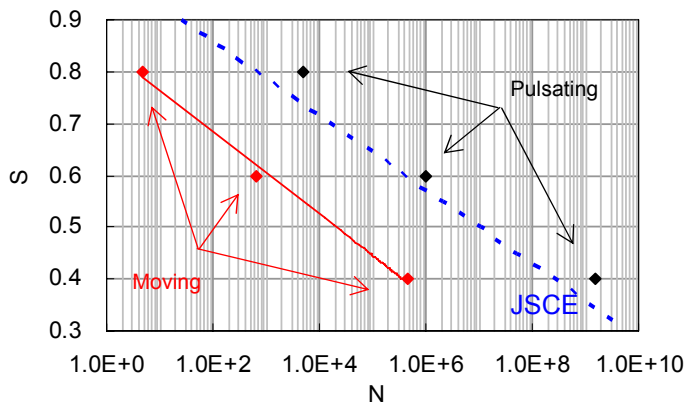
exists while changing its direction (figure 3.5 and 3.6). It means that once cracking occurs, rough crack surface is always under reversal cyclic shear. It accelerates damaging of surface interlock, and shear transfer mechanism across crack is deteriorated. Consequently slab loses stiffness and fail.

The fact which was pointed out in experimental studies is confirmed in this simulation as well.

3.3 Effects of design specification

Generally, it is known that a thick slab has longer life than a thin slab. In the same way, we can say something about reinforcement arrangement and
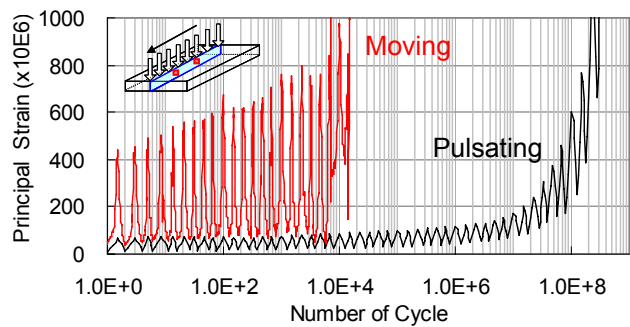

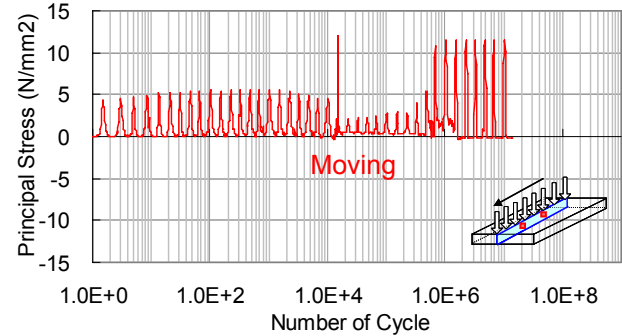Figure 3.4 Principal strains at the referential finite element concerned

Figure 3.2 Progress of mid-span deflection

Figure 3.5 Principal stresses at the referential finite element concerned
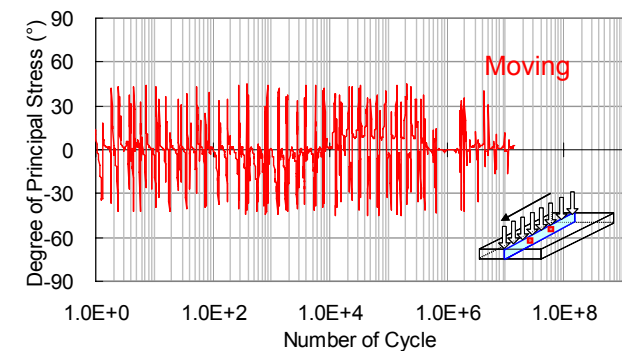

Figure 3.3 S-N diagrams for prototype

Figure 3.6 Direction of Principal stresses

prestressing force. However, it is difficult to qualitatively point out effects. The authors aim to build the evaluation method for practical use and parametric studies are performed.

First, slab thickness is examined with 30mm thicker or thinner slab models as compare to the prototype. Here, the amount of reinforcement is fixed. After fatigue simulation under moving loads, results are plotted on S-N diagram (figure 3.7). It is apparent that the ultimate capacity increases in proportion to the slab thickness. When the diagrams are normalized by the static capacity (figure 3.8), unique S-N intrinsic diagram can be seen regardless of the slab thickness. Accordingly, the effect of thickness can be treated simply for practice.

Second, the effect of reinforcement arrangement is investigated. The slab thickness is fixed the same as the prototype of 190mm. Table 3.3 provides models to compare and their reinforcement ratio. RC2 has smaller amount of longitudinal reinforcement. This is based on former code. Isotropic slab RC3 follows basic concept of CHBDC. RC4 is one way slab. This might be said extreme case.

Static capacities of this series are listed on table 3.4. The response to reinforcement arrangement seems not to be sensitive, even though it includes one way slab. Also S-N diagram normalized by each static capacity does not show noticeable difference under this research conditions. The results indicate that in case of ideal slabs which is not affected by initial defects such as cracking due to drying shrinkage, the influence of reinforcement arrangement is not so significant. It is widely accepted that reinforcement arrangement controls initial cracking, in such a meaning reinforcement arrangement might have influence to the fatigue life of RC slabs.

Pre-stressing effect is argued as the third interest. In this study, pre-stressing level is described by

$P = \sigma_p / f'_c$. σ_p is the pre-stressing stress and f'_c is compressive strength of concrete. To assess the effect of pre-stressing, compressive forces in the transverse direction are applied to the slab directly without any device. Also other conditions such as
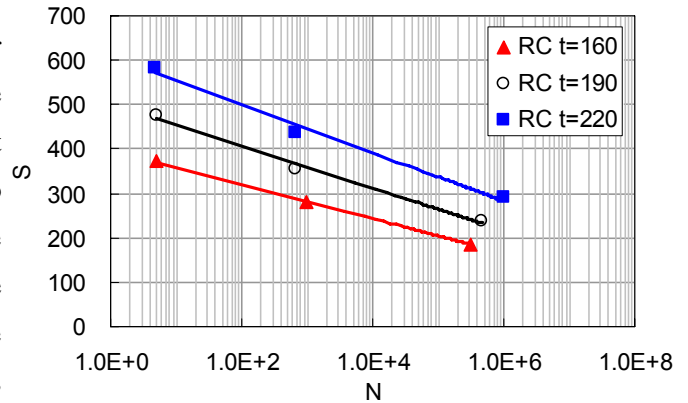

Figure 3.7 S-N diagram for comparison of slab thickness (absolute capacity)
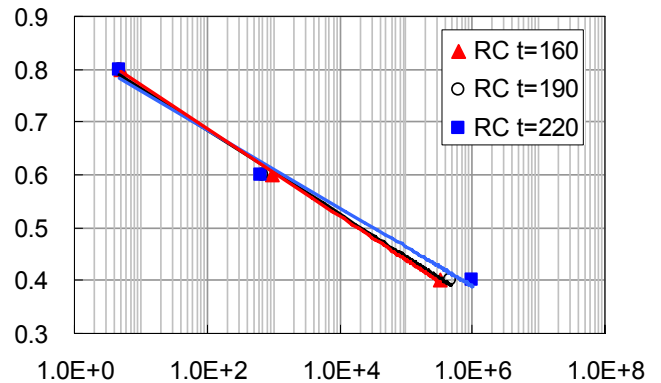

Figure 3.8 Normalized S-N diagram in terms of slab thickness

Table 3.3 Reinforcement ratio for comparison of reinforcement arrangement

Case	Transverse (Main)	Longitudinal (orthogonal)
Prototype RC1	0.0106 (0.0054)	0.0080 (0.0040)
Reduce RC2	0.0106 (0.0054)	0.0026 (0.0014)
Isotropic RC3	0.0070 (0.0070)	0.0070 (0.0070)
One way RC4	0.0106 (0.0054)	0.0000 (0.0000)

Table 3.4 Static capacity in relation to reinforcement arrangement

Case	Pmax (kN)	δ (m)	$P_{arrange}$ / $P_{original}$
RC1	594.03	0.0077	1.00
RC2	582.01	0.0083	0.98
RC3	560.01	0.0086	0.94
RC4	559.55	0.0081	0.94

thickness, reinforcement arrangement and material strength are kept the same.

The results obtained from static analysis are presented in table 3.5. Associated with pre-stressing force, an increase of ultimate capacity corresponding to reduced mid-span deflection can be observed. Cross section of RC1 and PCT1 at the maximum loading is shown in figure 3.9. In transverse section normal to the traffic direction, different types of deformation are observed. It might be said that flexural deformation is dominant rather than the shear in case of PCT1.

Figure 3.10 is a normalized S-N diagram. Interestingly, the slope is different between RC1 and other cases although there is no remarkable difference among PC cases. According to the former finding, it can be said that pre-stress is one of the most effective methods to prolong fatigue life, especially low stress - high cycle area. In contrast, the pre-stressing effect is not correlated with the level of pre-stressing force according to current investigation. A possible explanation for this limitation might be that relatively breakable direction normal to pre-stressing force becomes

criterion of failure regardless the value of pre-stressing. By using simulation, the effective boundary might be identified for each slab.

Here, one question is raised on the direction of pre-stressing. Table 3.6 and figure 3.11 show the comparison of prestressing directions. PCL1 is subjected compressive force along the traffic direction. 2PCTL1 is subjected pre-stressing in both
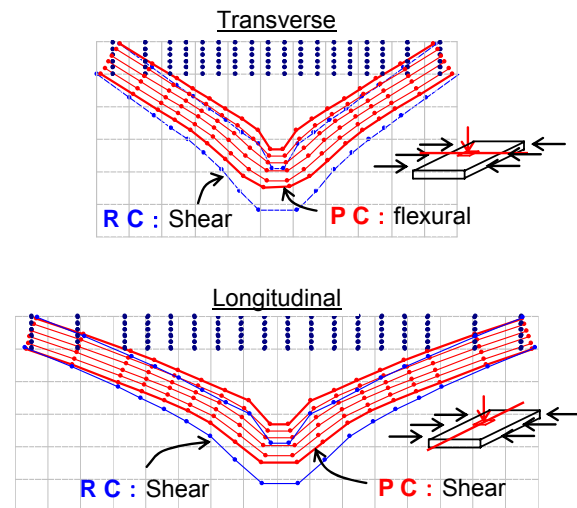

Figure 3.9 Cross section at the maximum load
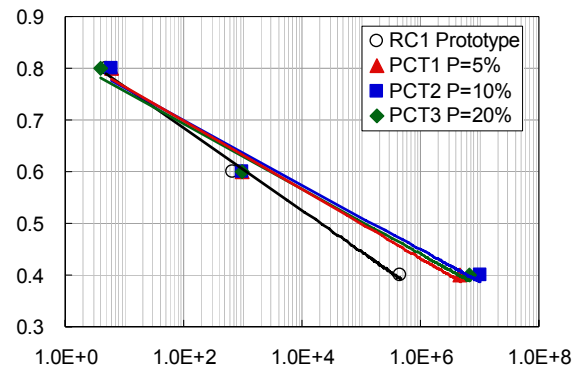

Figure 3.10 Normalized S-N diagrams in terms of pre-stressing forces
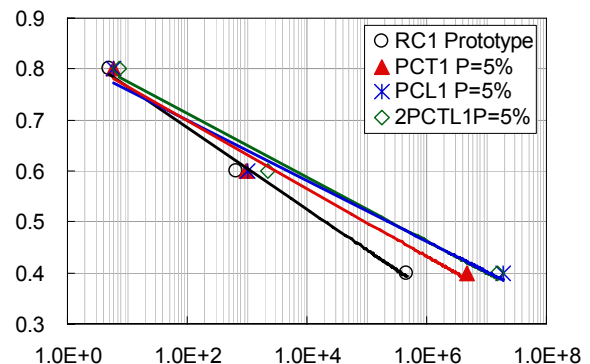
Figure 3.11 Normalized S-N diagrams regarding the pre-stressing directions

Table 3.5 Static capacity in relation to the pre-stressing forces

Case	Pmax (kN)	δ (m)	$P_{arrange} / P_{original}$
RC1	594.03	0.0077	1.00
PCT1 P=0.05	601.28	0.0064	1.01
PCT2 P=0.10	620.74	0.0059	1.04
PCT3 P=0.20	667.71	0.0058	1.12

Table 3.6 Static capacity in relation to the pre-stressing directions

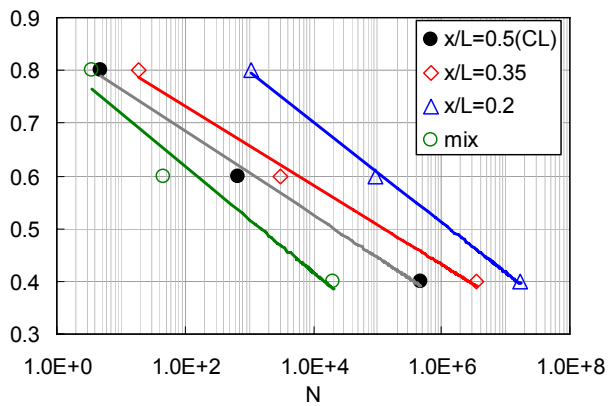| Case	Pmax (kN)	δ (m)	$P_{arrange} / P_{original}$
RC1	594.03	0.0077	1.00
PCT1 P=0.05	601.28	0.0064	1.01
PCL1 P=0.05	586.03	0.0064	0.99
2PCTL1 P=0.05	624.79	0.0064	1.05

Figure 3.12 Normalized S-N diagrams for offset loading effect
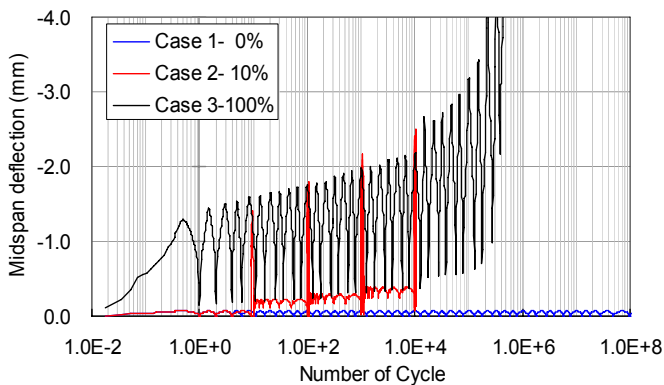
Figure 3.14 Mid-span deflections in comparison with heavy traffic.

X/L=0.20

X/L=0.35

Figure 3.13 Failure modes for offset effect

directions. If we focus on the fatigue life under the moving load (figure 3.11), PCL1 and 2PCTL1 successfully extend the life rather than PCT1. These results may encourage the explanation of failure mechanism under the moving load as shown in **3.2**.

3.3 Effects of traffic conditions

Traffic condition has direct influence on fatigue life of slab. The relationship between loading lane and span length is expressed with index X/L. X/L=0.5 means traffic runs on the centre line of slab. Fatigue life of X/L=0.2, 0.35, 0.5(CL) and mixed case are shown in figure 3.12. X/L=0.35 seems similar result to CL, however there is a clear difference between these two and X/L=0.2. Figure 3.13 indicates the answer through comparison of their failure mode. Only X/L=0.2 occurs local failure.

Mixed case may happen in practice. One thing confirmed in this study is that offset-type loading reduces fatigue life of slab especially low stress case.
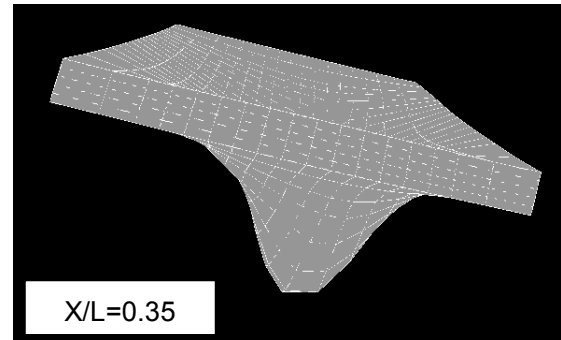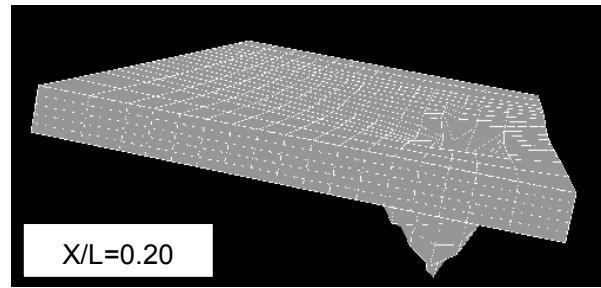
This result suggests that fatigue life strongly depends on both road plan and arrangement of main structure.

The heavy traffic ratio is also one of the measures affecting fatigue life. In this study, two types of traffic load are assumed. One is 20(kN) based on the weight of ordinary cars, another is 250(kN) that means a whole weight of a trailer. To compare the effect of traffic variation simply, contact area is fixed. Figure 3.14 provides mid-span deflection of three cases. Case 1 means ordinary car only, case 2 means ordinary traffic including 10% heavy trailer and case 3 is only heavy traffic load. Noteworthy, in case 2, the amplitude of mid-span deflection between heavy traffic seems almost same level as case 3. It can thus be suggested that heavy traffic has major influence to the fatigue life of bridge deck slabs

4. THE EFFECT OF WATER

4.1 Simulation on the effect of water

Previous studies by Matsui (1987) has shown that water tremendously reduces fatigue life of bridge deck slabs under moving loads. A recent study by Maekawa *et al.* (2006) computationally reproduced

reduced fatigue life coupled with water.

As shown in figure 2.1, computational system consists of core three constitutive models. Among them, the compression constitutive model has an option to consider the reduced concrete fatigue strength in water. The reduction rate is defined based on the experimental facts, and proposed alternative fatigue damage accumulation factor denoted by λ mathematically as,

$$\lambda = K_c^3 \cdot (1 - K_c)^4 \cdot g \cdot R - - - Air$$
$$\lambda = 100 \cdot (1 - K_c) \cdot g \cdot R - - - Water$$

In case of the crack shear transfer model, a phenomenological indicator ξ_w was installed by Gebreyouhannes (2006) as,

$$\tau = X \cdot \tau_0(\delta/\omega)$$
$$X = 1 - \frac{1}{10} \log_{10} \left\{ 1 + \int \left| d\left(\xi\xi_w \frac{\delta}{\omega} \right) \right| \right\}$$

The value ξ_w is around 10 extracted from experiments. In addition, the enhanced model which may treat both statically submerged and flowing water conditions was proposed in the current study (Gebreyouhannes 2008). This approach is based on both experimental result and physical consideration of crack shear mechanism. In the fully submerged condition, maximum local compressive strength of rough crack surface is decreased. It means that shear carried by aggregate interlocking is declined. The other hand, under down ward water, not only interface fracture but also shear slip is accelerated because of washing out crashed particles within crack. This phenomena is expressed as ξ_w is around 10~100. By combining these enhanced models, fatigue simulation with water is conducted in **4.2**.

4.2 Fatigue simulation with enhanced crack shear transfer model in water

A simple beam model is adopted for examining enhanced crack shear transfer model in water (figure 4.1). The pulsating load amplitude is 0-50kN and 50kN is 55% of ultimate capacity. Mid-span deflection progress under the pulsating load is shown in figure 4.2. Fatigue life in dry condition is almost 3 times longer than others. There is no significant difference between submerged case and flow case. However another tendency is observed in the case of
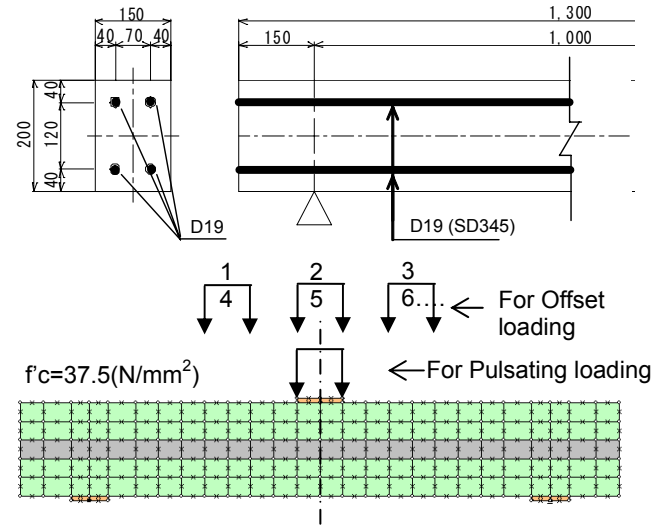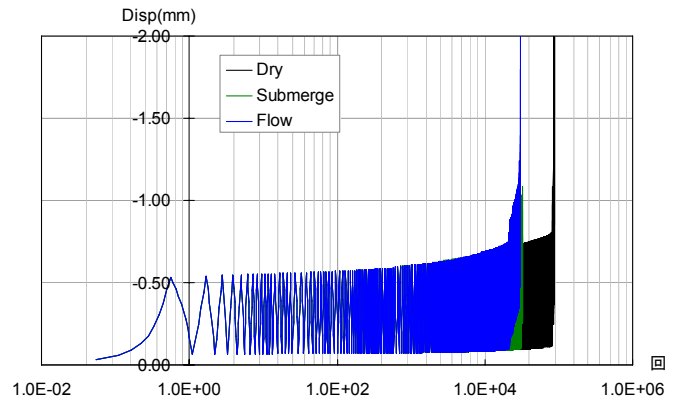

Figure 4.1 A simple beam model

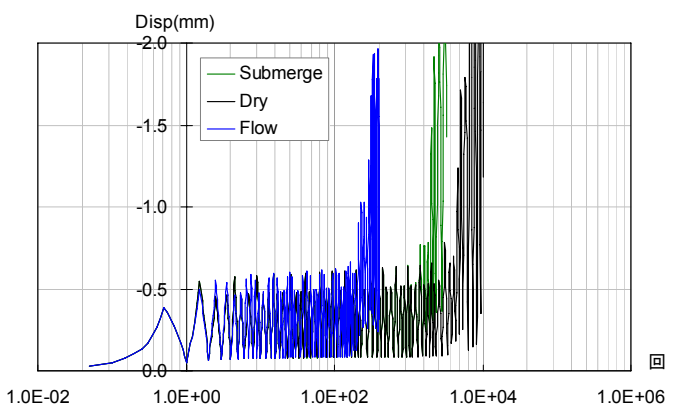Figure 4.2 Mid-span deflections in progress under pulsating load

Figure 4.3 Mid-span deflections in progress under traffic offset loading

offset loading (figure 4.3). The effect of wash out crashed particle within crack by water seems relatively large as compare to the difference between dry condition and submerged condition. It might be said that shear transfer is dominant in case of offset point fatigue loading.

5. CONCLUSIONS

The fatigue life of RC bridge deck slab under moving load is successfully simulated with full 3D nonlinear finite element analysis with the path dependent constitutive modeling. Through the sensitivity analysis, fatigue life related factors are presented that has never been quantitatively verified experimentally. For practical use, effects of water, traffic patterns and prestressing should be verified carefully by experiments in future. The authors are tackling to investigate environmental effects with initial defects, and is currently under discussion.

This study presents possibility to estimate some unknown risks related to life of infrastructures and to propose some countermeasures to maintain existing facilities with damages and defects.

REFERENCES

E. Gebreyouhannnes, Shear transfer of cracked concrete under fatigue loading, *Proceedings of 6th, international PhD Symposium in Civil Engineering*, fib, Zurich, 2006

E. Gebreyouhannes, Local-contact damage based modeling of shear transfer fatigue in cracks and its application to fatigue life assessment of reinforced concrete structures, ph.D thesis the University of Tokyo, Japan, 2008.

Maekawa, K., Pimanmas, A. and Okamura,H., 2003. *Nonlinear Mechanics of Reinforced Concrete*, Spon Press, London.

Maekawa,K., Toongoenthong, K., Gebreyouhannes, E. and Kishi, T. 2006a. Direct path-integral scheme for fatigue simulation of reinforced concrete in shear, *Journal of Advanced Concrete Technology*, Japan, 4(1):159-177.

Maekawa, K., Gebreyouhannes, E., Mishima, T. and X. An, 2006. Three-dimensional fatigue simulation of RC slabs under traveling wheel-type loads, *Journal of Advanced Concrete Technology*, Japan, 4(3):445-457.

Y. Maeda and S. Matsui, Fatigue of reinforced concrete slabs under trucking wheel load, *Proceedings of JCI*, Japan, 6, pp. 221 - 224, 1984

S. Matsui, Fatigue strength of RC-slabs of highway bridge by wheel running machine and influence of water on fatigue, *Proceedings of JCI*, Japan, 9(2), pp. 627-632, 1987

Pedikaris, P.C. and Beim, S.R., 1989. RC bridge decks under pulsating and moving load, *Journal of Structural Engineering*, ASCE, 114(3):591-607.

Pedikaris, P.C., Beim, S.R. and Bousias, S.N., 1989. Slab continuity effect on ultimate and fatigue strength of reinforced concrete bridge deck models, *Structural Journal*, ACI, 86(4):483-491.